A lateral belt of cortical LGN and NuMA guides mitotic spindle movements and planar division in neuroepithelial cells

Elise Peyre,[1] Florence Jaouen,[1] Mehdi Saadaoui,[1,3] Laurence Haren,[2] Andreas Merdes,[2] Pascale Durbec,[1] and Xavier Morin[1,3]

[1]Université de la Méditerranée/Aix-Marseille II, Developmental Biology Institute (IBDML), Centre National de la Recherche Scientifique UMR6216, Case 907, Campus de Luminy, 13288 Marseille, France
[2]CNRS-Pierre Fabre, 31400 Toulouse, France
[3]Ecole Normale Supérieure, Institut de Biologie de l'ENS, IBENS, Paris, Inserm U1024, Paris, F-75005 France

To maintain tissue architecture, epithelial cells divide in a planar fashion, perpendicular to their main polarity axis. As the centrosome resumes an apical localization in interphase, planar spindle orientation is reset at each cell cycle. We used three-dimensional live imaging of GFP-labeled centrosomes to investigate the dynamics of spindle orientation in chick neuroepithelial cells. The mitotic spindle displays stereotypic movements during metaphase, with an active phase of planar orientation and a subsequent phase of planar maintenance before anaphase. We describe the localization of the NuMA and LGN proteins in a belt at the lateral cell cortex during spindle orientation. Finally, we show that the complex formed of LGN, NuMA, and of cortically located Gαi subunits is necessary for spindle movements and regulates the dynamics of spindle orientation. The restricted localization of LGN and NuMA in the lateral belt is instructive for the planar alignment of the mitotic spindle, and required for its planar maintenance.

Introduction

Oriented cell divisions are essential for the development, growth, and homeostasis of many tissues. In epithelia, most divisions occur within the plane of the tissue (Fleming et al., 2007). This contributes to the expansion of the tissue's surface, and is also essential for tissue cohesion and maintaining the epithelial monolayer organization: failure to orient the spindle properly may result in unequal distribution of polarized cell junctions between sister cells, leading to loss of attachment and to exit of one sister from the monolayer and possibly deleterious effects (Morin et al., 2007; Jaffe et al., 2008; Fleming et al., 2009; Zheng et al., 2010). In the chick embryonic neuroepithelium, defective planar orientation leads to increased proliferation of misplaced neuroepithelial cells (Morin et al., 2007). Within epithelial sheets, coordinated orientation of cell divisions may contribute to tissue elongation along a specific axis (Baena-López et al., 2005). During mammalian kidney development, failure to orient divisions along the axis of the renal tubules results in tubular enlargement and polycystic kidney disease (Fischer et al., 2006). Asymmetric cell divisions rely on extrinsic or intrinsic cues to produce progenies with a different identity, and orientation of the mitotic spindle can play a crucial role in both cases. For example, stem cells in the *Drosophila* male germline orient their axis of division to maintain one of the progeny in contact to an environmental self-renewal signal, while the other daughter cell is born away from this signal and differentiates (Yamashita and Fuller, 2008). In fly embryonic and larval neuroblasts, coordination between the polarized, asymmetric distribution of intrinsic cell fate determinants and the orientation of the axis of division of the mother cell is crucial to resolve differential cell fates (Cabernard and Doe, 2009).

There are two main strategies to achieve a specific spindle orientation (Yamashita and Fuller, 2008). The orientation may

Correspondence to Xavier Morin: xavier.morin@ens.fr

Abbreviations used in this paper: Gαi, inhibitory alpha subunit of heterotrimeric G protein; LGN, leucine-glycine-asparagine repeat protein; NuMA, nuclear and mitotic apparatus.

The Rockefeller University Press $30.00
J. Cell Biol. Vol. 193 No. 1 141–154
www.jcb.org/cgi/doi/10.1083/jcb.201101039

be fixed before mitosis and inherited throughout the cell cycle from one division to the next, like in the *Drosophila* male germline in which the centrosome is trapped next to the cell cortex after division. After duplication, one centrosome remains in the same position while the other is free to wander away, and the spindle forms in its definitive orientation, with one pole tethered to the cell cortex. This is a convenient way for these cells to divide asymmetrically repeatedly and to keep the self-renewing cell in the same position in the stem cell niche. A similar behavior has been described in asymmetrically dividing neuroblasts of the *Drosophila* embryonic and larval nervous system, with the notable exception of the first division of the lineage in the embryo (Rebollo et al., 2007, 2009; Rusan and Peifer, 2007). However, other cell types divide in a different orientation from one cell cycle to the next, or need to relocate their centrosome in interphase. This is the case in ciliated epithelial cells, which divide in a planar manner, but whose centrosome forms the base of the apical cilium during interphase. In these cells, the mitotic spindle tends to form with a random orientation and planar orientation is achieved by rotation of the assembled mitotic spindle during metaphase (Reinsch and Karsenti, 1994; Roszko et al., 2006). Rotation is driven by cortical forces exerted on astral microtubules emanating from the spindle poles (Théry et al., 2007). The minus end–directed motor activity of the dynein–dynactin complex, combined with cortical anchoring of the complex, generates pulling forces on astral microtubules (Busson et al., 1998; Nguyen-Ngoc et al., 2007; Siller and Doe, 2008; Yingling et al., 2008). Local differences in cortical forces attract spindle poles toward stronger pulling forces and result in spindle rotation.

We and others have previously shown that the G protein regulator leucine-glycine-asparagine repeat protein (LGN) is necessary for planar spindle orientation in chick and mouse neuroepithelial cells (Morin et al., 2007; Konno et al., 2008). A recent study has shown a role for LGN in symmetric planar divisions and epithelial morphogenesis in a model of cyst formation (Zheng et al., 2010). LGN contains four C-terminal GoLoco domains that directly interact with GDP-bound inhibitory α-subunits of heterotrimeric G proteins (Gαi1, Gαi2, and Gαi3 in vertebrates, and to a lesser extent Gαo; Siderovski et al., 1999). Its N terminus contains seven TPR (tetratricopeptide repeat) domains, the second of which interacts with the nuclear and mitotic apparatus protein (NuMA; Du et al., 2001, 2002). Both interactions are necessary for LGN to perform its function in vertebrate epithelial cells (Morin et al., 2007; Zheng et al., 2010). This molecular cassette (hereafter called the LGN complex) appears to regulate spindle orientation by linking astral microtubules to the cell cortex, as NuMA interacts with microtubules and with the dynein–dynactin motor complex (Merdes et al., 1996, 2000) and Gαi subunits are anchored to the cell membrane by myristoylation. Invertebrate counterparts of the Gαi–LGN–NuMA complex (respectively Gα–GPR1/2–lin5 in *C. elegans* and Gαi–Pins–Mud in *Drosophila*) have been involved in regulating axial spindle orientation in a number of models of asymmetric divisions, including the nematode zygote and fly neural progenitors (Bellaiche and Gotta, 2005). The LGN complex therefore appears as a general regulator of oriented cell divisions, in model systems showing either reset (vertebrate epithelial cells) or inherited (*Drosophila* larval neuroblasts) spindle orientation.

In this paper, we investigate the dynamics of spindle orientation in chick neuroepithelial cells. We show that it follows a stereotypic three-dimensional pattern during metaphase, with an active phase of planar spindle orientation and a subsequent phase of planar maintenance. We then investigate the distribution of members of the LGN complex in neuroepithelial cells and show that LGN and NuMA localize in a lateral belt at the cell cortex during cell division. Finally, we show that the LGN complex is necessary for the biphasic spindle movement pattern and regulates the dynamics of spindle orientation. Its restricted localization in the lateral belt is instructive for planar spindle alignment and required for planar maintenance. Knockdown or mislocalization of members of the LGN complex results in spindle orientation defects, which ultimately lead to disorganization of the neuroepithelium. These data identify Gαi, LGN, and NuMA as essential regulators of mitotic spindle dynamics, planar cell division, and epithelial organization in vertebrate cells in vivo.

Results

A biphasic movement leads to planar orientation of the mitotic spindle in neuroepithelial cells

The vertebrate neuroepithelium is organized as a pseudo-stratified monolayer of elongated, proliferative cells, which constitute the initial reservoir of neural stem cells. 80–90% of these cells divide in the plane of the neuroepithelial apical surface (Noctor et al., 2008; Shioi et al., 2009). Planar orientation of the mitotic spindle ensures the symmetric parting of the apical membrane and subapical junctions and is essential to maintain the monolayered organization (Morin et al., 2007). Several studies have reported highly dynamic movements of the mitotic spindle during metaphase in murine and chick neural progenitor cells (Adams, 1996; Haydar et al., 2003; Roszko et al., 2006; Morin et al., 2007), but none combined sufficient temporal and spatial resolution to accurately represent spindle movements in space.

We used in ovo electroporation in the E2 chick embryo to label the centrosomes and/or chromosomes of neuroepithelial cells with chick Centrin2-GFP and human Histone2b-GFP fusion proteins, respectively. Electroporated neural tubes were harvested at E3 and cultured en face, with their apical surface facing the coverslip. 3D stacks of confocal images were acquired at 1-min intervals for several hours (Fig. S1; Video 1). As a consequence of interkinetic nuclear movements, all cells undergoing mitosis have their mitotic spindle located immediately underneath the apical surface and can be imaged in the same field close to the coverslip, with the Z axis corresponding to the apical–basal axis of the cell. Using the 3D coordinates of spindle poles, we can measure the orientation and movements of the spindle between successive time points (see Materials and methods). α_Z is the angle of the axis of the spindle relative to the apical surface and α_{XY} is the angle of the projection of the spindle axis on the XY plane relative to its initial value at metaphase

onset (determined as described in the Materials and methods section). Temporal variations in α_Z and α_{XY} values indicate movements of rotation of the mitotic spindle relative to the apical–basal axis (Z-rotation) and within the apical plane (XY-rotation), respectively. We analyzed a cohort of 37 Centrin2-GFP–labeled cells taken from 6 independent experiments. Fig. 1, a and b, and Videos 2 and 3 show a representative time-lapse sequence of a single Centrin2-GFP cell imaged from the apical surface (Fig. 1 a; Video 2) and seen as a Z-section along its mitotic spindle axis (Fig. 1 b; Video 3).

While α_Z was random at the onset of metaphase, all cells quickly aligned their spindle with the apical surface ($\alpha_Z < 30°$) and maintained this planar orientation until anaphase onset (Fig. 1, b–d; Video 3). The average time for planar spindle alignment was less than 5 min (Fig. 1, b, d, and f), whereas metaphase lasted on average 23.16 ± 0.7 min. Remarkably, after they had reached a planar orientation, all mitotic spindles maintained an active XY-rotation (Fig. 1, a and e; Video 2). The dynamics of this XY-rotation appears random and most cells change the direction of their XY-rotation at least once during metaphase. Fig. 1 d and e show the time course of α_Z and α_{XY} during metaphase for several representative examples, and the full dataset is presented in Fig. S2. The average deviation in XY-orientation during metaphase (defined as the value of α_{XY} at anaphase onset) was 82.2 ± 13°, ranging from 1° to a full rotation (353°) (Fig. S2), suggesting that the final orientation of the divisions within the neuroepithelial plane is independent from its initial position. It is also independent from the dorso–ventral and antero–posterior axes (Fig. S2, Video 4). Interestingly, the average speed of spindle rotation increased ∼5 min after metaphase onset, corresponding to the time when all spindles have reached a planar orientation (Fig. 1 g). As this phenomenon was also observed in cells whose initial spindle orientation was planar (0–30° relative to the apical surface, $n = 10$ cells), this acceleration is likely to depend on metaphase progression rather than on the apical–basal orientation of the spindle (Fig. S2).

Overall, these data show that mitotic spindle orientation follows a biphasic stereotypic pattern: during early metaphase, the spindle is actively driven to quickly orient parallel to the apical surface. During late metaphase and until anaphase, it is maintained in this planar orientation while being free to revolve randomly around the apico–basal axis, as summarized in Fig. 1 h and Video 5.

LGN and NuMA localize at the lateral cell cortex during cell division

Members of the LGN complex and their invertebrate homologues have been involved in cortical force generation in different cell types. In particular, in invertebrate models of asymmetric cell division, polarized distribution of the complex dictates the positioning of one spindle pole and controls spindle orientation at anaphase. We therefore investigated their distribution in dividing neuroepithelial cells. All three Gαi subunits are expressed in the chick spinal cord (Fig. S3, a and b). As staining with anti-Gαi1/2 subunit antibody produced an indistinct punctuate signal (not depicted), we used the weak CMV promoter to drive low level expression of a YFP-tagged human Gαi1 subunit (Du and Macara, 2004) in chick neuroepithelial cells and observed a uniform distribution of Gαi1 at the cell cortex during metaphase and anaphase (Fig. 2, a, b, and g). A cortical enrichment of LGN has been described over the spindle poles in dividing progenitors of the E14.5 mouse telencephalon and in cultured MDCK cysts (Konno et al., 2008; Zheng et al., 2010). Using a chick LGN-GFP fusion protein and 3D en face imaging in E3 chick embryos, we found that LGN actually forms a homogeneous ring on the lateral cortex of metaphase and anaphase neuroepithelial cells and is absent from the apical and basal cortex (Fig. 2, c, d, and h). After planar alignment and in anaphase, the poles of the mitotic spindle are located underneath this ring. This distribution is only observed when GFP-LGN is expressed at very low levels. High expression levels lead to cortical saturation and cytoplasmic enrichment of the GFP signal (Fig. S3 c). Finally, using a monoclonal antibody directed against chick NuMA, we found that NuMA also forms a ring on the lateral cell cortex of dividing progenitors and is absent from the more apical and basal regions (Fig. 2, e–h). NuMA is also detected on the distal regions of the mitotic spindle, just underneath the spindle poles, as was previously described in cell culture (Merdes et al., 2000).

The lateral distribution of LGN and NuMA depends on Gαi-GDP but not on aPKC

Biochemical studies in invertebrate and vertebrate species show that LGN directly interacts with NuMA via its N-terminal TPR (tetratricopeptide repeat) domain region (Du et al., 2001, 2002), and with Gαi-GDP subunits via its C-terminal GoLoco domains (Willard et al., 2004). We found that expressing high levels of the wild-type and of the constitutive GDP-bound G203A point mutant form of rat Gαi1(Willard et al., 2004) dramatically increases the cortical recruitment of LGN-GFP, which is now homogeneously distributed around the cell cortex from basal to apical locations (Fig. 3 a). Under these conditions, high levels of LGN-GFP can be expressed without saturation of the cortical recruitment (Fig. S3 d). By contrast, expression of the constitutive GDP-bound G213A point mutant of Gαolf subunit has no effect on GFP-LGN subcellular distribution (Fig. 3 a), consistent with the fact that GoLoco domains specifically bind GDP-bound members of the Gαi subfamily (Willard et al., 2004).

Knockdown of LGN and expression of the C-terminal GoLoco domains of LGN, which compete with full-length LGN for Gαi-GDP interaction and prevent its cortical distribution (Morin et al., 2007), both prevent the cortical localization of NuMA, although NuMA is still detected on spindle poles (Fig. 3 b). By contrast, knockdown of NuMA does not abolish the cortical distribution of LGN (Fig. 3 c).

In an MDCK epithelial cyst model, LGN is similarly restricted to the lateral cortex of dividing cells despite the presence of apical Gαi subunits (Hao et al., 2010). In this model, direct phosphorylation of a serine residue at position 401 of LGN by apically localized atypical protein kinase C (aPKC) increases its affinity for the 14-3-3 protein (Hao et al., 2010) and inhibits the Gαi–LGN interaction, causing LGN removal from the apical cortex. To test whether the same mechanism

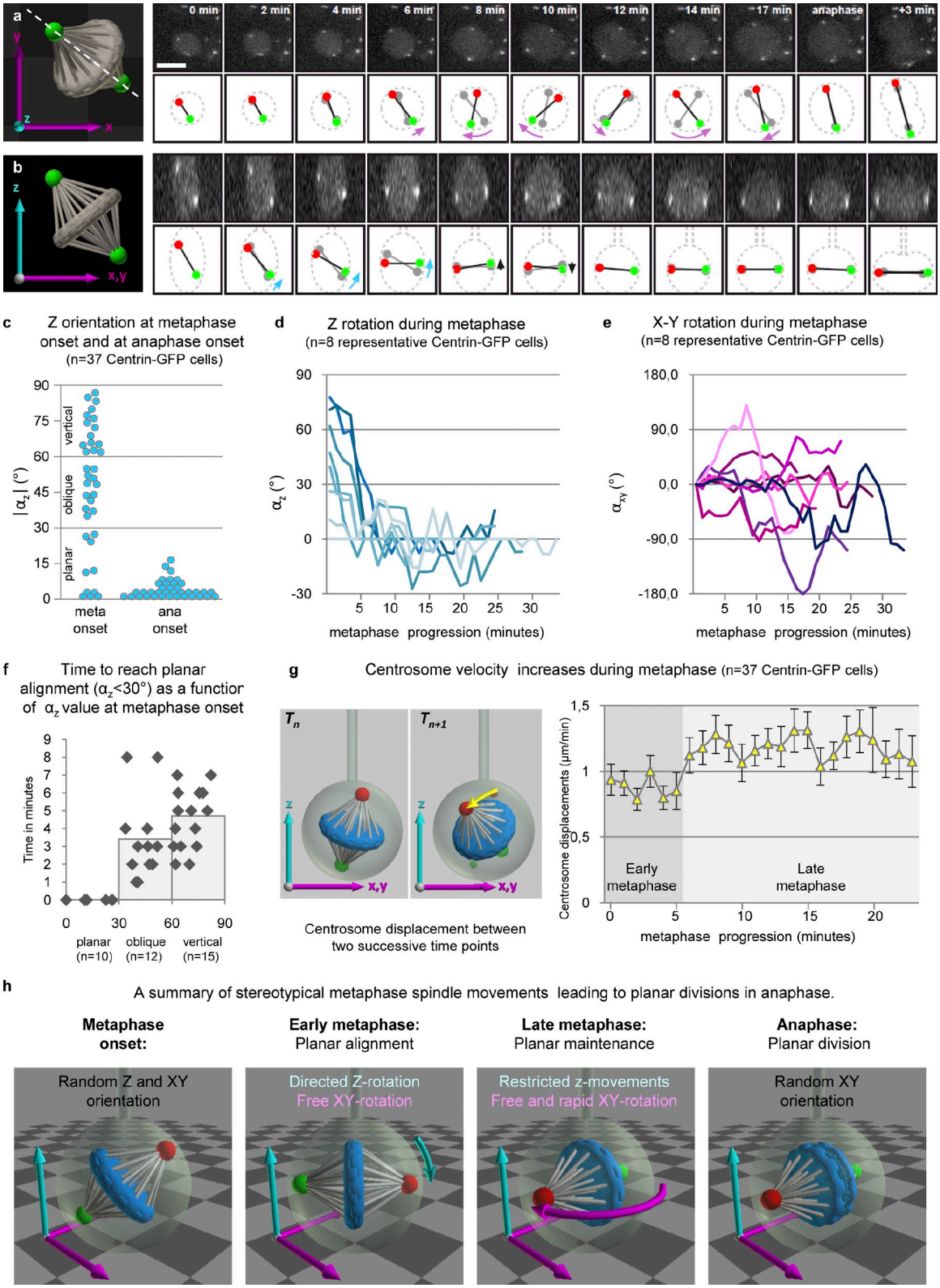

Figure 1. **3D time-lapse imaging shows stereotypical biphasic movements of the mitotic spindle in neuroepithelial cells.** (a and b) Time-lapse series of a Centrin2-GFP–expressing neuroepithelial cell in metaphase and anaphase. (a) Top row: successive apical projections of a 20-µm-thick Z-stack; bottom row: a schematic of the XY orientation of the spindle at each time point (colored spindle poles) relative to the previous time point (gray spindle poles). Purple arrows indicate the orientation of the movement between time points and reveal numerous changes in orientation during metaphase. (b) Top row: the same cell as in panel a is seen as successive vertical Z-sections along the axis of the mitotic spindle. Bottom row: a schematic of the same sections. Blue arrows indicate the rotation of the spindle relative to the apical/basal (Z) axis between successive time points. Note that within 6 min the spindle, starting from an oblique position, has aligned with the apical surface and remains aligned until anaphase. Left: 3D models of a metaphase neuroepithelial cell imaged from the apical surface (XY plane) or seen along its apical–basal axis (Z axis) are provided. Bar, 5 µm. (c) The orientation of the spindle relative to the apical

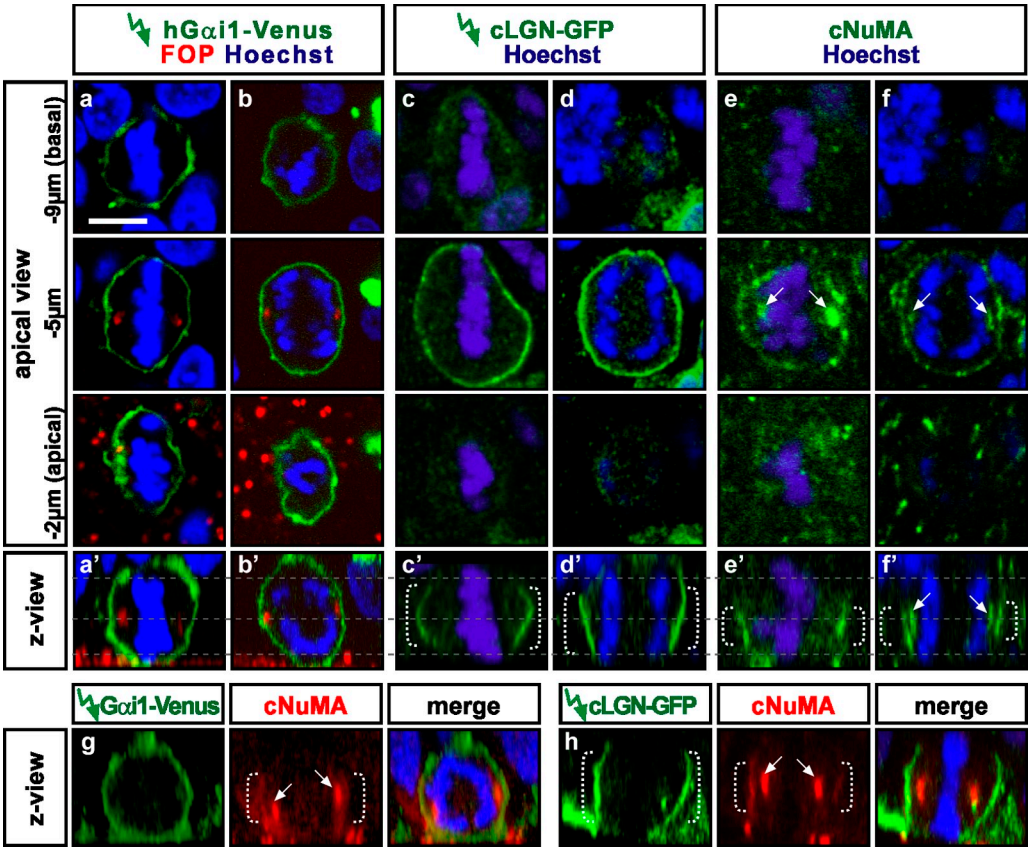

Figure 2. **Gαi, LGN, and NuMA distribution in dividing neuroepithelial cells.** (a–b′) Gαi-Venus (green) shows a homogenous cortical distribution in metaphase (a–a′) and anaphase (b–b′) cells. The three panels in a and b show single optical sections from basal (top) to sub-apical (bottom) levels, whereas a′ and b′ show a Z-view of the same cell. FOP (red) labels centrosomes. (c–d′) LGN-GFP (green) is excluded from the apical and basal cortex in metaphase (c–c′) and anaphase (d–d′) neuroepithelial cells, and forms a wide belt at the lateral cortex. (e–f′) NuMA (green) is excluded from the apical and basal cortex in metaphase (e–e′) and anaphase (f–f′) neuroepithelial cells, and forms a narrow belt at the lateral cortex. Note that f–f′ shows the same cell as d–d′. (g) Double staining for Gαi-Venus (green) and NuMA (red) show the restricted expression of cNuMA at the lateral cortex, whereas Gαi is homogeneous at the cortex. (h) Double staining for LGN-GFP (green) and NuMA (red) shows restricted expression of both proteins at the lateral cortex. Lightning arrows indicate the electroporated product. Bar, 5 µm

is used to restrict LGN to the lateral cortex of chick neuroepithelial cells, we expressed a constitutively activated, myristylated form of aPKC (Zheng et al., 2010) together with LGN. LGN is still observed at the cell cortex (Fig. 3 d). Conversely, when the neuroepithelium is cultured in presence of an aPKC inhibitor, LGN is still restricted to the lateral cortical domain (Fig. 3 e). Finally, we compared the distribution of wild-type LGN to a mutant version in which the serine residue 401 is mutated to an alanine. The mutant protein is poorly recruited to the cell cortex compared with wild-type LGN. However, a lateral enrichment remains detectable in dividing progenitors (Fig. 3 f). Taken together, these data suggest that, contrary to MDCK cells, apical aPKC may be neither sufficient nor necessary to exclude LGN from the apical cortex in dividing neuroepithelial cells.

Restricted localization of LGN and NuMA in the lateral domain controls planar spindle orientation

The specific localization of LGN and NuMA on the lateral cortex of dividing cells is compatible with a role of these molecules in regulating planar spindle positioning (Video 6), and we have shown that LGN is necessary for planar spindle orientation in neuroepithelial cells (Fig. 4 a; Morin et al., 2007). We tested whether NuMA and Gαi subunits cooperate with LGN for spindle orientation. Knockdown of NuMA as

surface (α_Z) is random at metaphase onset (left), but by anaphase onset all the spindles have adopted a planar orientation parallel to the apical surface (right). (d) Dynamics of Z orientation (α_Z) during metaphase: all cells in our study quickly align their spindle parallel to the apical surface during the first minutes of metaphase and remain aligned until anaphase. Eight representative cells are shown. (e) Dynamics of xy orientation (α_{XY}) during metaphase: all cells exhibit active and random XY rotation throughout metaphase. The eight cells are the same as in panel b. (f) The time needed for the spindle to reach a planar orientation depends on its initial Z-orientation. (g) Centrosome velocity from 37 Centrin2-GFP+ cells during metaphase shows an inflection between 5 and 7 min. Error bars = SEM. (h) A 3D schematic of the successive movements of the spindle during metaphase. Immediately after metaphase onset, the spindle quickly undergoes a directed Z-rotation leading to planar orientation; Z rotation is then restricted to maintain planar orientation and most of the movement occurs randomly in a plane parallel to the apical surface. Throughout this figure, blue, magenta, or yellow represent movements and their measurements along the Z axis, in the XY plane, and in the three dimensions, respectively.

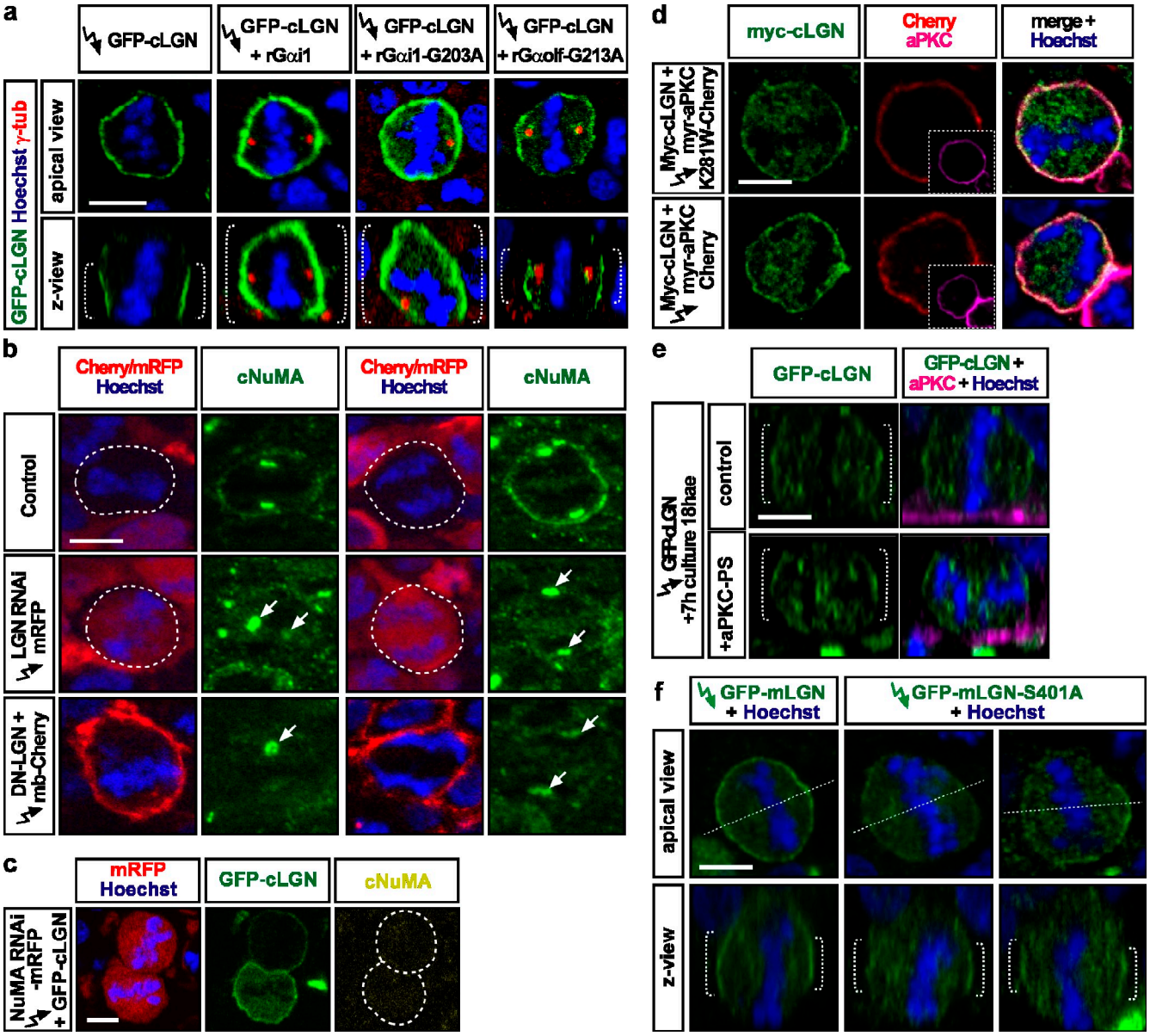

Figure 3. **The lateral distribution of LGN and NuMA is regulated by Gαi-GDP and not by aPKC.** (a) GDP-bound Gαi-subunits recruit LGN-GFP to the cell cortex. Apical (top) and Z (bottom) views of cells expressing LGN-GFP fusion protein alone or in combination with Gαi1, Gαi1-GDP, or Gαolf-GDP. LGN-GFP recruitment is increased and expanded along the apical–basal axis upon Gαi and Gαi-GDP expression. (b) NuMA is recruited to the cell cortex by LGN. Cells expressing LGN RNAi hairpin or dominant-negative LGN do not show cortical NuMA in metaphase and anaphase. Note that NuMA is still present at the spindle poles (arrows). (c) Two metaphase cells expressing a NuMA RNAi hairpin: NuMA knockdown does not prevent LGN cortical recruitment. (d) Overexpression of a ubiquitous cortical, activated form of aPKC does not inhibit LGN cortical recruitment compared with an inactive mutant version (K281W) of myristylated aPKC. (e) Inhibition of aPKC with a myristylated pseudo-substrate does not block apical exclusion of GFP-LGN. (f) Replacement of the aPKC phosphorylation site (serine 401) by an alanine residue does not block the apical exclusion of GFP-tagged mouse LGN. All images are apical views, except panel e and the bottom rows in panels a and f, which are Z-views showing the apico–basal distribution of LGN. Lightning arrows indicate the electroporated product(s). Bar, 5 µm.

well as double knockdown of Gαi1 and Gαi2 subunits by RNA interference caused subtle but significant spindle orientation defects (Fig. 4 a). Treatment with pertussis toxin (PTx) was recently shown to prevent the membrane targeting of Gαi subunits in Hela cells (Woodard et al., 2010). Accordingly, expression of the catalytic subunit of PTx (PTx-A) disrupted planar spindle orientation in E3 neuroepithelial cells (Fig. 4 b).

We then tested whether the restricted distribution of LGN and NuMA to the lateral cortex is important for precise spindle positioning. Gαi1-G203A expression, which redistributes LGN homogeneously around the whole cell cortex, caused a complete randomization of spindle orientation in anaphase (Fig. 4 c).

We observed that all conditions which perturb spindle orientation at E3 result in the production of ectopic neural progenitors in the mantle zone 24 h later (Table I). This phenotype can be explained by the unequal inheritance of apical attachments during cytokinesis of dividing neuroepithelial cells and delamination of one of the sister cells, which does not inherit these attachments but retains a progenitor identity, as previously

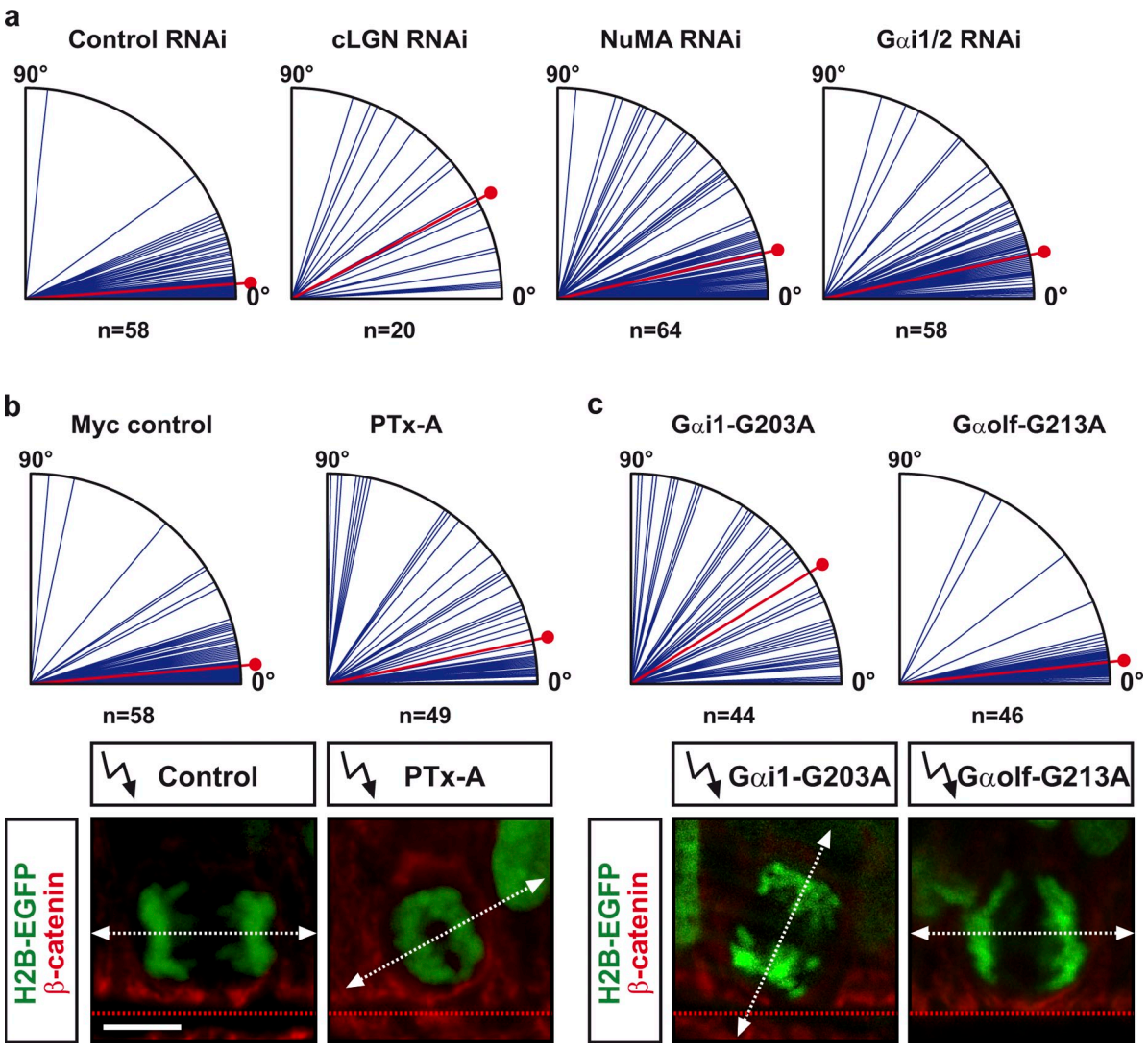

Figure 4. **The lateral LGN complex is required for planar cell division.** (a) Spindle orientation in anaphase was measured at E3 in transverse sections of the neural tube 24 h after electroporation. Knockdowns of LGN, NuMA, and Gαi1/2 result in defects in spindle orientation compared with a control RNAi construct targeting luciferase. (b) Top: treatment with the pertussis toxin catalytic subunit (PTx-A) randomizes spindle orientation compared with electroporation with a control Myc-tag expressing vector. Bottom: representative cells with spindle orientation defects in anaphase. H2B-GFP (green) reveals the parting chromosomes in anaphase, β-catenin (red) shows the cell outline and apical surface. (c) Overexpression of Gαi-GDP (Gαi-G203A) results in spindle randomization, whereas Gαolf-GDP (Gαolf-G213A) has no effect. Solid red line in graphs: median angle. Significance was assessed using the Kolmogorov-Smirnov test. There was no significant difference between control conditions (Myc, miLuc, and Gαolf-G213A). All other conditions differed significantly from the controls. *n* represents the number of measured cells. Data are collected from at least five embryos for each condition. Lightning arrows indicate the electroporated product(s). Bar, 5 µm.

described for LGN loss of function (Morin et al., 2007). Expression of a cytosolic form of Gαi1, thought to compete with endogenous cortical Gαi for LGN cortical recruitment, mimicked LGN knockdown and led to ectopic neural progenitors in the chick neural tube (Table I), consistent with the observation that it causes abnormal spindle orientation and defective cystogenesis in a 3D MDCK cyst culture model (Zheng et al., 2010). Expression of Gαi2, Gαi3, and Gαtransducin, which have all been shown to interact with LGN GoLoco domains with affinities similar to Gαi1, all led to the same phenotype (Table I). By contrast, expression of wild-type or GDP-bound versions of Gαolf did not cause any such defect (Table I), consistent with the observation that Gαolf-G213A (Gαolf-GDP) had no effect on spindle orientation (Fig. 4 c).

Gαi-GDP–dependent distribution of NuMA and LGN at the lateral cortex is both instructive and permissive for spindle movements

We used live imaging of spindle poles to compare the dynamics of spindle movements between wild-type cells and several different mutant conditions that lead to spindle orientation defects (Fig. 5 a). In cells expressing high levels of Gαi-G203A, the spindle moved freely and randomly in the three dimensions throughout metaphase. Remarkably, it could pass through a planar orientation several times during metaphase, but did not stabilize there and went on rotating relative to the apico–basal axis until anaphase onset (Fig. 5, b and c; Video 7). Overall, spindle rotation movements increased by 50% upon Gαi-G203A

Table I. **Summary of the effect of different gain and loss-of-function constructs on LGN and NuMA distribution, spindle orientation, and production of ectopic neural progenitors**

Condition	LGN distribution[b]	NuMA distribution	Spindle orientation	Ectopic progenitors at E4[c]
Wild type	Lateral cortical ring	Cortical ring/spindle poles	Planar	–
LGN RNAi	–	No ring/spindle poles	Random	++[a]
Ct-LGN	Cytoplasmic[a]	No ring/spindle poles	Random[a]	++[a]
LGN RNAi + mLGN rescue	ND	ND	Planar (wild type)[a]	–[a]
NuMA RNAi	Cortical	–	Defects	+
Gαi1/2 RNAi	ND	ND	Defects	+
PTx-A	ND	ND	Defects	++
ratGαi1-G203A	Strong cortical	No ring/faint cortical?/spindle poles	Random	++
ratGαi1	Strong cortical	ND	ND	++
Cyto-ratGαi1	ND	ND	ND	++
ratGαi2	ND	ND	ND	++
ratGαi3	ND	ND	ND	++
Human Gαtransducin	ND	ND	ND	++
ratGαolf	ND	ND	ND	–
ratGαolf-G213A	Cortical (wild type)	ND	Planar (wild type)	–

ND, not determined.

[a]Morin et al, 2007.

[b]Data from overexpression of GFP-tagged chick LGN or Myc-tagged mouse LGN.

[c]Ectopic progenitors are determined by the presence of BrdU+ cells in the mantle zone on transverse sections at E4 after a 45-min BrdU pulse (see Morin et al, 2007).

expression (Fig. 5 g). In contrast, spindle rotation was greatly reduced in cells where NuMA or LGN levels had been knocked down by RNA inhibition, as well as in cells expressing the dominant-negative C-terminal domain of LGN (Fig. 5, d–g; Video 8; Morin et al., 2007). In these cells, the mitotic spindle mostly oscillated around its initial position. A residual oriented movement was visible in some NuMA RNAi cells, although much slower than in wild-type cells, so that some cells eventually reached a near-planar spindle orientation before anaphase (Fig. 5 d). This correlates with the mild defects in spindle orientation observed in fixed tissues (Fig. 5 a) and might be explained by residual NuMA activity: while cells treated with NuMA RNAi do not show any detectable NuMA signal with our antibody, Q-RT-PCR analysis indicates only 85% reduction in NuMA mRNA levels (Fig. S4). Together, analyses in live cells indicate that the Gαi-GDP–dependent recruitment of LGN and NuMA at the cell cortex is necessary for spindle movements. In wild-type cells, the lateral distribution of the LGN complex is instructive to direct the initial planar alignment of the spindle and permissive for the ensuing random 2D movement constrained by the lateral ring.

Discussion

In this study, we used live 3D imaging to investigate the dynamics of mitotic spindle movements leading to planar cell division in chick neuroepithelial cells. To achieve high 3D resolution, we labeled the centrosomes with a Centrin2-GFP fusion protein and used en face imaging of the whole neuroepithelium to obtain reproducible space coordinates. With this method, we show that planar orientation of cell divisions in the neuroepithelium is achieved through a biphasic movement of mitotic spindle orientation, involving a first phase of oriented spindle rotation toward a planar orientation and a second phase of planar maintenance, during which the spindle is free to revolve within the plane of the tissue. We show that Gαi subunits, LGN, and NuMA all play a role in this movement and control the final planar orientation of neuroepithelial cell division. In particular, we demonstrate that LGN and NuMA localize in restricted domains of the cell cortex, forming a lateral cortical belt that determines the final position of spindle poles at anaphase. Based on invertebrate models (Nguyen-Ngoc et al., 2007), biochemical data (Merdes et al., 1996), and recent observations in cultured cells in vitro (Woodard et al., 2010), it is likely that NuMA recruits the dynein–dynactin complex to the lateral cortex and that this complex exerts pulling forces on astral microtubules that contact this cortical region. A higher concentration of the complex at the lateral cell cortex would generate stronger pulling forces on astral microtubules, and result in the attraction of both spindle poles toward the lateral cortex. This would cause a rotation of the mitotic spindle toward a planar orientation in early metaphase and later help maintain this planar orientation until anaphase. In the absence of LGN or NuMA, spindle rotation is strongly reduced (Video 8), although occasionally one cell displays rapid random rotation (Fig. 5, e and f). The distribution of the LGN complex as a lateral ring suggests that cortical forces exerted through astral microtubules on spindle poles are homogeneously distributed throughout the lateral cortex. This might be permissive for the random movements of spindle rotation observed after planar orientation is achieved. Accordingly, upon expression of Gαi-G203A, when LGN is relocated homogeneously throughout the cortex, spindle movements are more intense and their orientation becomes random. In particular the spindle can pass through a planar orientation several times during metaphase and does not stop there (Fig. 5, b and c). This suggests that the ring of LGN and NuMA may be the only cue for planar spindle orientation.

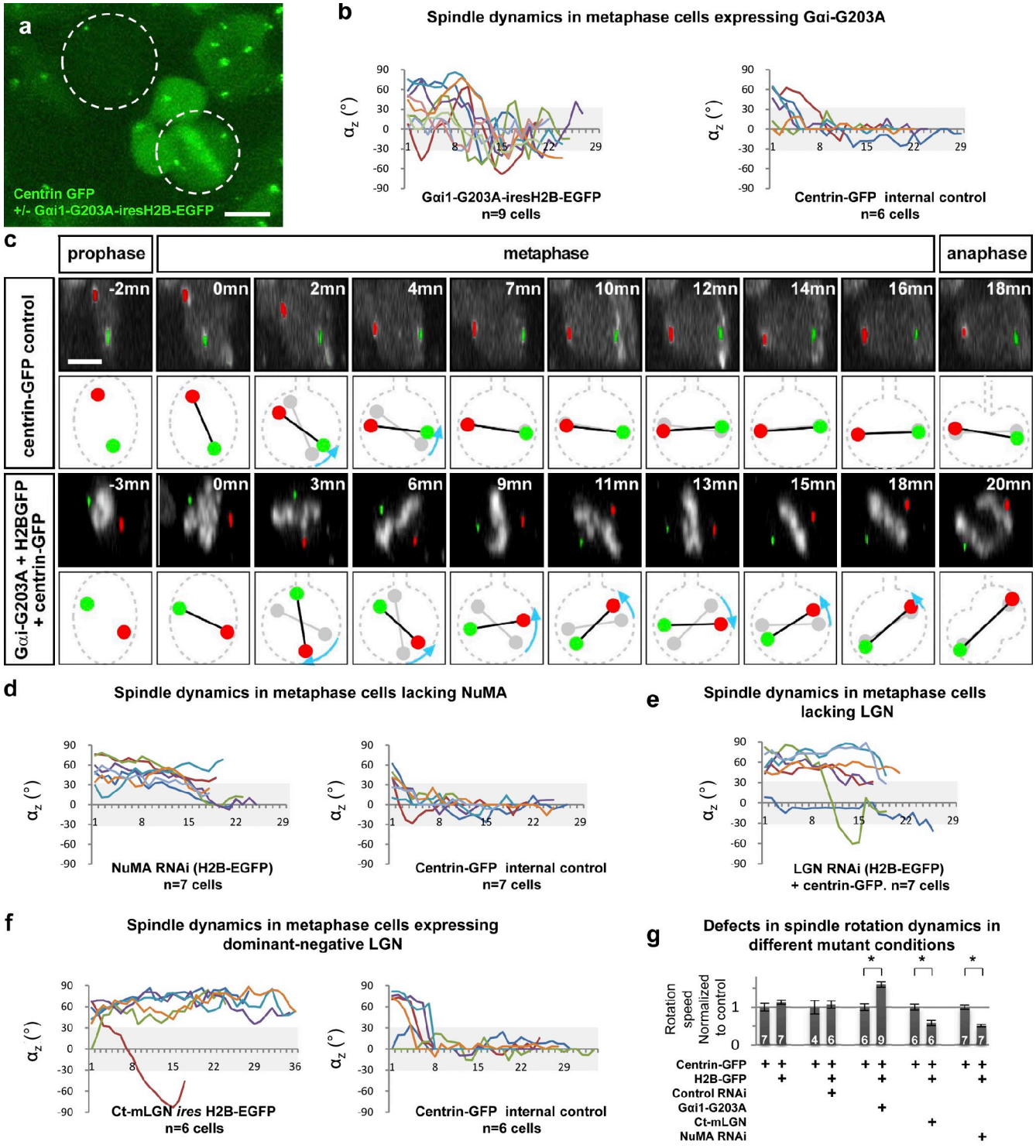

Figure 5. **The lateral LGN complex controls the stereotypical dynamics of spindle movements.** (a) Still image from a time-lapse movie showing a metaphase wild-type cell expressing Centrin2-GFP only in the same field as a mutant cell expressing Centrin2-GFP + high levels of Gαi-G203A-ires-H2B-GFP (see Materials and methods). (b) Time-course of the spindle α_Z variations during metaphase indicates systematic random movements upon Gαi-G203A expression (left graph) compared with quick planar orientation of Centrin2-GFP–expressing control cells (right graph) from the same field. (c) Time-lapse analysis of spindle movements relative to the apico–basal axis in a control Centrin2-GFP (top) and a Gαi-G203A-ires-H2B-GFP + Centrin2-GFP–expressing cell (bottom), taken from the same field in the same embryo. Apical is at the bottom and Centrin2-GFP–expressing centrosomes are pseudo-colored in red and green. In the control cell, most of the Z rotation (blue arrows) occurs within the first minutes of metaphase and is directed toward planar orientation. In the Gαi-G203A–expressing cell, Z rotation occurs throughout metaphase and is randomly oriented, and anaphase occurs with a random oblique axis. (d–f) Spindle Z-rotation is decreased by reduction of NuMA (d) or LGN (e) levels with RNAi and by expression of a dominant-negative form of LGN (f). (g) Global spindle dynamics during metaphase increases when Gαi-G203A increases, and decreases in the absence of cortical LGN and NuMA. Each pair of bars compares the average dynamics of mutant cells to Centrin2-GFP–expressing cells in the same field, in the same embryo (see Materials and methods). Numbers in the bars indicate the number of cells analyzed for each genotype. Spindle dynamics was not changed by expression of H2B-GFP or a control RNAi hairpin directed against luciferase. Error bar = SEM, *, $P < 0.01$; unpaired student *t* test. Bar, 5 µm.

Remarkably, live analysis in mutant conditions shows that defects in spindle rotation and orientation do not delay anaphase onset (unpublished data), indicating that there is no spindle orientation checkpoint before anaphase. Hence, a rapid rotation during the first minutes of metaphase ensures that the planar orientation is safely achieved long before anaphase onset.

Homologues of the LGN complex play a role in spindle orientation in invertebrate models of asymmetric division (Gönczy, 2008). In these divisions, asymmetric fate in the progeny relies on the coordination of the axis of division with the polarized distribution of cell fate determinants to ensure their unequal segregation between sister cells. Accordingly, LGN complex homologues are observed as a polarized crescent that determines a fixed axial orientation for the spindle (apico–basal in *Drosophila* embryonic neuroblasts, antero–posterior in *C. elegans* zygotes and fly larval sensory organ precursors). By contrast, in epithelial cells, the distribution in a lateral ring offers one degree of freedom, which allows for the random orientation of divisions within the 360° of the neuroepithelial surface plane (Fig. S2).

The LGN complex appears as a generic molecular machinery used to link the cell cortex to astral microtubules, which can be deployed in a different manner depending on the cell type and its particular developmental needs for oriented cell divisions. In this respect, it will be interesting to follow the distribution of the LGN complex in epithelial tissues whose polarized growth depends on oriented planar divisions, such as mammalian renal tubules (Fischer et al., 2006).

Cortical anchoring of LGN is an essential prerequisite for its function in all cell types and it relies on the Gαi–GoLoco domain interaction (Yu et al., 2002; Morin et al., 2007; Zheng et al., 2010). However, LGN localization at the cortex needs to be further refined for precise spindle orientation. This can be achieved either by local recruitment or by local exclusion. One case of local recruitment is the *Drosophila* neuroblast, in which the LGN complex is recruited apically via the direct interaction between Pins and Inscuteable; in Insc mutant neuroblasts Pins and Gαi are redistributed homogeneously at the cortex and apical–basal spindle orientation is disrupted (Yu et al., 2000; Schaefer et al., 2001), while ectopic expression of Inscuteable indeed forces Pins–LGN to the apical cortex and induces apico–basal spindle reorientation in several epithelial cell types (Yu et al., 2000; Konno et al., 2008; Poulson and Lechler, 2010). By contrast, in MDCK epithelial cells, it was shown that LGN is actively excluded from the apical cortex by aPKC phosphorylation (Hao et al., 2010; Zheng et al., 2010). Our data suggest that neuroepithelial cells use a different mechanism for the apical exclusion/lateral enrichment of LGN, raising two questions: why would these two epithelial cell types use a different mechanism, and how is LGN restricted to the lateral cortex?

MDCK cells are epithelial cells of kidney origin. When cultured under appropriate conditions, these symmetrically dividing and exponentially growing cells display an extremely robust and stable epithelial organization. By contrast, in vivo, neuroepithelial cells represent a transient developmental stage. They dramatically remodel their apical–basal organization at the onset of neurogenesis (Aaku-Saraste et al., 1997; Costa et al., 2008), during which they perform both symmetric and asymmetric divisions to give rise to differentiated progeny. Indeed, in our hands, several molecules shown to specifically address a GFP fusion apically in MDCK cells fail to do so in chick neural progenitors (unpublished data). Hence, some aspects of the regulation of apical–basal polarity, possibly extending to the regulation of planar spindle orientation, are differentially regulated between the two cell types. As most epithelial cell types, both in vivo and in vitro, predominantly use planar divisions, it will be important to study how much conservation and divergence exist between different models to regulate this phenomenon.

High levels of LGN overexpression lead to its cytoplasmic accumulation (Fig. S3) without causing any significant spindle orientation defects (Morin et al., 2007), whereas increasing cortical Gαi concentration increases the cortical recruitment of LGN, bypasses its lateral restriction, and leads to random spindle orientation. This suggests that: (a) physiological Gαi-GDP concentrations are permissive but limiting for the cortical recruitment of LGN and NuMA; (b) LGN and Gαi-GDP subunits can exert their role on spindle orientation only when they interact at the cell cortex; and (c) LGN–Gαi-GDP interactions are controlled and limited to the lateral cortex. There are several alternative mechanisms for the lateral enrichment of LGN. Polarized distribution of guanine exchange factors (GEFs), GTPase accelerating proteins (GAPs), or guanine dissociation inhibitors (GDIs) could bias the Gαi-GTP vs. Gαi-GDP balance and modulate LGN distribution along the apico–basal axis. Similarly, apical enrichment of Gβγ subunits may sequester Gαi-GDP and prevent apical LGN accumulation. However, neither overexpression of LGN, nor expression of Gβ sequestrating agents, such as Gαolf-G213A or the C-terminal domain of β-adrenergic receptor kinase (Ct-βARK), did perturb spindle orientation (Morin et al., 2007; Fig. 5 c and unpublished data). Besides, Sanada and Tsai (2005) have described a cortical enrichment of Gβ, if any, over spindle poles in mouse cortical progenitors, and they reported more planar divisions upon Ct-βARK overexpression. The polarity regulator LKB1 can phosphorylate LGN and its orthologue AGS3 in their C-terminal region, where Gαi-GDP interaction domains (GoLoco domains) are located (Blumer et al., 2003). Although the LKB1 phosphorylation site was not identified, the same study indicated that phosphorylated GoLoco domains have a reduced affinity for Gαi-GDP. LKB1 localizes subapically in mouse radial glial cells at E15 (Barnes et al., 2007) and was described at the level of subapical junctions and in the apical cilium in MDCK cells (Sebbagh et al., 2009; Boehlke et al., 2010), although its expression and localization were not described during mitosis in these cells. Local phosphorylation of LGN by apically localized LKB1 might reduce the affinity of LGN for Gαi-GDP subunits and prevent its apical accumulation. Alternatively, LGN might be directly targeted to the lateral cortex through its interaction with basolateral polarity regulators of the DLG family (Sans et al., 2005). It is not yet possible to discriminate between these possibilities, and detailed studies on the dynamics of the cortical distribution of LGN and its many known interactors are needed.

In neuroepithelial cells, the apical surface and subapical attachment sites only represent 2% of the dividing cell surface (Kosodo et al., 2004). We have previously shown that equal partitioning of subapical attachment sites is essential to maintain the two sister cells within the ventricular zone (Morin et al., 2007). In this study, we observe that even mild defects in spindle orientation, such as those caused by partial Gαi1-2 RNAi, NuMA RNAi, or PTx expression (Fig. 5), are probably sufficient for the unequal segregation of apical attachment sites because they systematically result in the production of misplaced progenitors in the mantle zone (Table I). This emphasizes the strict requirement for a very precise planar spindle positioning to maintain tissue architecture in the neuroepithelium.

Materials and methods

Electroporation

Electroporation was performed in E2 chick embryos as described previously (Morin et al., 2007). Typically, vectors for gain and loss of function were used at a concentration of 2 µg/µl. Vectors that do not carry a fluorescent reporter were supplemented with an H2B-GFP– or GFP-expressing vector at 1 µg/µl. A list of all the vectors used in this study is presented in Fig. S5. Full detail of vector construction and sequences can be obtained from X. Morin upon request. Sequences used to target chick LGN, NuMA, Gαi1, and Gαi 2 for knockdown are: LGN-192: 5′-GAATACCATCACCATGATTTA-3′ (Morin et al., 2007); NuMA-1152: 5′-CAGGAGAAGAAATGCCTAGAA-3′; NuMA-3995: 5′-GATGACCATCGAGGCACTGAA-3′; Gαi1-174: 5′-GCTGGTTATTCAGAAGAAGAA-3′; and Gαi2-189: 5′-GAGGAGTGCCGGCAATACAAA-3′. For the simultaneous analysis of wild-type and mutant cells in live experiments (Fig. 5), we generated vectors carrying a loxP-flanked PolyA sequence between the CAGGS promoter and a bicistronic messenger carrying either Ct-mLGN or Gαi-G203A followed by H2B-GFP (Fig. S5). These vectors were electroporated at 2 µg/µl together with a Centrin2-GFP–expressing vector (1 µg/µl). Addition of a Cre recombinase-expressing vector at a concentration of 100 ng/µl typically resulted in excision of the PolyA and expression of Ct-mLGN (or Gαi-G203A) and H2B-GFP in approximately half of the Centrin2-GFP–positive cells. For RNAi experiments, two electroporations were performed at 6-h intervals in the same embryos, the first one with the RNAi vector carrying the H2B-GFP reporter (2 µg/µl) supplemented with the Centrin2-GFP vector (1 µg/µl) and the second one with the Centrin2-GFP vector (1 µg/µl) alone. Embryos were harvested for live imaging 18 h after the second electroporation and regions showing both single Centrin2-GFP and double Centrin2-GFP/H2B-GFP cells were used for analysis.

Immunohistochemistry and in situ hybridization

The full-length sequence of chick NuMA cDNA has been deposited into the GenBank/EMBL/DDBJ nucleotide sequence database under accession no. FN994986. For the production of monoclonal antibodies against NuMA, cDNA encoding amino acids 1698–2141 of chicken NuMA was cloned into pRSET-B plasmid (Invitrogen) and expressed in BL-21 bacteria. The 6His-tagged NuMA protein was extracted with 8 M urea in 50 mM sodium phosphate, pH 7.9, and purified over nickel-sepharose. The purified protein was dialysed against 20 mM $NaHCO_3$ and injected into BALB/c mice. Spleens of mice that showed an immune response were fused with P3-X63Ag8 myelomas and culture supernatants of positive clones were screened on dot blots of NuMA fusion protein as well as by immunofluorescence in DU249 cells. The anti–chicken NuMA antibody was used at a 1:20 concentration in PBT (0.3% Triton X-100), 10% FCS, on embryos fixed for 2 h in 4% formaldehyde. In addition to the nuclear signal in interphase and to the cortical and spindle localization, a staining is observed on apical cilia. This ciliary staining is nonspecific, as it is not lost upon NuMA RNAi treatment, and is not observed upon expression of a NuMA-GFP fusion protein, which recapitulates the other NuMA antibody signals. Mouse anti-GFP (#TP401; Biolabs) was used at 1:200 dilution. Immunohistochemistry and in situ hybridization on cryosections or whole mount were performed as described in Morin et al. (2007).

En face culture

Embryos were harvested in PBS at E3, 24 h after electroporation. After removal of extraembryonic membranes, embryos were transferred to 37°C F12 medium and slit along their midline from the hindbrain to the caudal end. The electroporated side of the neural tube was peeled off with dissection forceps and transferred in F12 medium to a glass-bottom culture dish precoated with a thin layer of 2% low melting agarose F12 medium. 200 µl of 1% agarose F12 medium (1x penicillin/streptomycin, 1 mM sodium pyruvate) preheated at 42°C was gently pipetted up and down several times to soak the neural tubes. Excess medium was then removed so that the neural tubes would flatten with their apical surface adhering to the bottom of the dish and an additional thin layer of agarose medium was then added on top. After agarose polymerization, the whole dish was covered with 3 ml liquid F12/PS/sodium pyruvate medium and transferred to 37°C for 1 h for recovery before imaging.

Image acquisition

Optical sections of fixed samples were obtained either on a confocal microscope (LSM 510; Carl Zeiss, Inc.) using a 100x (Plan Apochromat NA 1.4 oil immersion) objective and Zeiss AIM software (Fig. 2; Fig. 3, a and c), on a confocal microscope (LSM 710; Carl Zeiss, Inc.) using a 63x (Plan Apochromat NA 1.4 oil immersion) objective and Zeiss ZEN software (Fig. 3, d and e), on a confocal microscope (model SP5; Leica) using a 63x (Plan Neofluar NA 1.3 oil immersion) objective and Leica LAS software (Fig. 3 f), or on an upright microscope (Axioskop; Carl Zeiss, Inc.) equipped with the Apotome module and a 63x (Plan Neofluar NA 1.3 oil immersion) objective (Fig. 3 b) or an 40x (F.Fluar NA 1.3 oil immersion) objective (Fig. 4, b and c) using Zeiss Axiovision software. Z-views were generated with the Ortho tool in the Zeiss LSM Image Browser, except in Fig. 3 f, where they were generated in ImageJ. Spindle orientation measurements in anaphase cells in fixed tissue were performed as in Morin et al. (2007). For live imaging, en face cultures of Centrin2-GFP– and/or H2B-GFP–expressing embryos were imaged with a 40x oil (Plan Neofluar, NA 1.3; Carl Zeiss, Inc.) or water (c-Apochromat, NA 1.2; Carl Zeiss, Inc.) immersion objective, on an inverted microscope (Axiovert 200M; Carl Zeiss, Inc.) equipped with a spinning disk confocal head (CSU-10; PerkinElmer), a heating chamber, and a solid-state laser diode at 488 nm. 20–30-µm-thick Z-stacks (1-µm steps) were acquired at 1-min intervals for 3–5 h using MetaMorph software (Molecular Devices) and a CCD camera (CoolSnapHQ; Roper Scientific). Stack projections of individual cells (time series in Fig. 1 a) were obtained with the maximum projection tool in MetaMorph. Z-line projections (time series in Fig. 1 b and Fig. 5 c) were created with the "kymograph" tool in MetaMorph, by manually tracing a 120-pixel-long line spanning the two centrosomes for each time point. Line width was set to 7 pixels. Individual images were imported into Photoshop software (Adobe), and rescaled along the XY and Z axes. 3D drawings and animations (Videos 5–8) were done with Anim8or software.

Determination of metaphase and anaphase onset

In cells expressing both H2B-GFP and Centrin2-GFP, metaphase onset can be determined on the basis of chromosome condensation and the appearance of a metaphase plate. Typically, the distance between centrosomes stabilizes between 6.5 and 8.5 µm at that point and remains stable until anaphase (before metaphase onset, both centrosomes migrate basally; the distance between them is unstable and does not appear to follow any rule, as in some cases it is as low as 3 µm and in some others it is higher than 12 µm). For cells expressing Centrin2-GFP only, in the absence of chromosomal marker, the onset of metaphase was determined empirically as the time when the distance between centrosomes reaches a stable value between 6.5 and 8.5 µm.

3D measurements of spindle movements

For each analyzed cell, to reconstruct 3D spindle movements, pixel values of the x and y positions of both centrosomes (C1 and C2) were obtained manually using the "Measure Pixels" tool in MetaMorph. The Z-position was determined as follows: typically one centrosome can be seen on three successive Z-levels (e.g., 6, 7, and 8 µm), and the Z-value of the second level (7) is chosen; in cases where the centrosome is seen on four sections (e.g., 6, 7, 8, and 9 µm), the intermediate value between the second and third (eg, 7.5) was used. The values were then entered in a Microsoft Excel sheet and x-y, x-y-z distances (in µm) and angles (in degrees) in the XY plane and relative to the Z axis were calculated using the following formulas (see illustration in Fig. S1):

$$\Delta x = (x_{C2}\text{-}x_{C1}) * 0.317125 \text{ or } \Delta x = (x_{C2}\text{-}x_{C1}) * 0.1586;$$

$$\Delta y = (y_{C2}\text{-}y_{C1}) * 0.317125 \text{ or } \Delta y = (y_{C2}\text{-}y_{C1}) * 0.1586$$

Table II. **Primers used for RT-PCR**

Amplified cDNA	Left primer	Right primer
L27	5′-AAGCCGGGGAAGGTGGTG-3′	5′-GGGTGGGCATCAGGTGGT-3′
LGN	5′-GCTGAGAGGCACCTGGAGATC-3′	5′-GCGCTGGGAAGGCGGCTGTC-3′
Gαi1	5′-GTACGCAGCCCCTGCCGAGATG-3′	5′-CCTTCCTCTGCTGCTCCAGCT-3′
Gαi2	5′-GAGAAGATCGTGCACAGCCCC-3′	5′-GTGCGTCCTTGCCGCCCTCA-3′
Gαi3	5′-ATGACCTTGTCTTGGCCGAGG-3′	5′-CCGCAGCGCTCCGCTTTACC-3′
Gαo	5′-GCAGTACAAGCCAGTGGTCTACAGC-3′	5′-CCTGCTCCGTGGGCTGGTAGTC-3′
Gαs	5′-GGACAATCAGACCAACCGGC-3′	5′-GCCTTCCATCTCCACTTGCTG-3′

(0.317125 and 0.1586 represent the conversion factor from pixels into µm measured for a 40x objective, with acquisitions performed with the "binning 2" or "binning 1" settings in MetaMorph, respectively).

$$\Delta z = z_{C2} - z_{C1.}$$

x-y distance (distance between the Z-projections of the two centrosomes in the XY plane):

$$\Delta xy = \sqrt{(\Delta x^2 + \Delta y^2)}.$$

x-y-z distance (distance between the two centrosomes):

$$\Delta xyz = \sqrt{(\Delta x^2 + \Delta y^2 + \Delta z^2)}.$$

arctan(Δx;Δy) gives the angle of the spindle in the XY plane relative to the x axis . In Fig. 1 e and Fig. S2, the angle of the spindle in the XY plane is standardized to its value at metaphase onset (t0), and is calculated as:

$$\alpha_{XY} = \arctan(\Delta x;\Delta y) - \arctan(\Delta x_{t0};\Delta y_{t0}).$$

The angle relative to the Z axis:

$$\alpha_Z = \arctan(\Delta z;\Delta xy).$$

The total rotation of the spindle between two successive time points t and t+1 (Δα) is calculated as:

$$\Delta\alpha = \arccos[|(\Delta x_t * \Delta x_{t+1}) + (\Delta y_t * \Delta y_{t+1}) + (\Delta z_t * \Delta z_{t+1})| / \Delta xyz_t * \Delta xyz_{t+1}].$$

Spindle dynamics is the average rotation of the spindle per minute during metaphase; it is calculated as:

$$\sum_{t0 = \text{metaphase onset}}^{\text{anaphase onset}} \frac{(\Delta\alpha)}{T}$$

where T represents metaphase length for this cell. In Fig. 5 g, spindle dynamics was calculated for each control and mutant cell, and averaged in the mutant and control populations for each experiment. The values in the controls were standardized to 1 for each experiment.

Centrosome velocity [Z velocity (V_Z), XY velocity (V_{XY}), and total velocity (V)] represents the centrosome displacements between two successive time points at 1-min intervals. It is calculated as:

$$V_Z = (\alpha_{Zt+1} - \alpha_{Zt}) * [(\Delta xyz_t + \Delta xyz_{t+1})/4] * 2\pi/360;$$

$$V_{XY} = (\alpha_{XYt+1} - \alpha_{XYt}) * [(\Delta xy_t + \Delta xy_{t+1})/4] * 2\pi/360;$$

$$V = \Delta\alpha * [(\Delta xyz_t + \Delta xyz_{t+1})/4] * 2\pi/360.$$

For angle measurements presented in Fig. 2 g, a time-lapse movie of a projection of 25 µm Z-stack H2B-GFP–expressing cells (Video 4) was imported into Axiovision software (Carl Zeiss, Inc.) and the orientation of the mitotic spindle relative to the horizontal axis of the movie was measured using the angle measurement tool for the first 160 dividing cells in the movie.

RT-PCR

Total RNA was obtained from chick E3 trunks, E4 trunks, and E4 limbs using TRIzol reagent (Invitrogen) and following the manufacturer's instructions. cDNA was synthesized using Superscript III first strand synthesis kit (Invitrogen) and following the manufacturer's instructions. PCR was performed with 28 rounds of amplification (1 min at 94°C, 1 min at 53°C, and 1 min at 72°C) using pairs of primers specific for chick ribosomal protein L27 (control), Gαi1, Gαi2, Gαi3, Gαo, Gαs, and LGN genes. All fragments were between 250 and 400 bp. Primers used for RT-PCR are listed in Table II.

Evaluation of RNAi efficiency by quantitative RT-PCR

FACS sorting. To evaluate the efficiency of NuMA and Gαi RNAi knockdown, the electroporated portion of the neuroepithelium of 10 E3 chick embryos was dissected 24 hours after electroporation in phosphate-buffered saline (PBS; see En face culture section for details), incubated in 1 ml 1x trypsin-EDTA medium (Invitrogen) at 37°C for 5 min. Trypsin was inactivated with 1 ml 10% fetal bovine serum in F12 medium and cells were dissociated by pipetting up and down with a 1-ml cone. After centrifugation at 1,000 rpm for 5 min, the pellet was resuspended in 1 ml of cold PEB buffer (PBS, 0.5% BSA, and 5 mM EDTA) for FACS sorting. For each RNAi vector, 80,000–100,000 wild-type (GFP negative) and knockdown (GFP positive) cells were sorted using a BD FACSAria high-speed cell sorter.

Quantitative RT-PCR. Immediately after sorting, total RNA was prepared from each population using the RNeasyPlus RNA purification kit (QIAGEN). RNA quantity was assessed using the NanoDrop 1000 (NanoDrop Technologies). Two retro-transcriptions were performed using Superscript III first strand synthesis kit (Invitrogen) for each sample with equal quantity of RNA and then pooled together. Quantitative PCR was performed on a Iq5 cycler (Bio-Rad Laboratories) using SYBR GreenER SuperMIX (Invitrogen). Annealing temperature was optimized for each primer set and the PCR reactions were evaluated by melting curve analysis following the manufacturer's instructions and checked by electrophoresis. cGAPDH mRNA was amplified to ensure cDNA integrity and to normalize expression. Each quantitative PCR was performed in triplicate for each set of RNA preparation. Primers used for Q-RT-PCR reactions are listed in Table III.

Online supplemental material

Fig. S1 shows the experimental set-up for 3D live imaging of chick neuroepithelial cells. Fig. S2 shows analysis of 3D dynamics of spindle rotation in wild-type Centrin2-GFP–expressing chick neuroepithelial cells. Fig. S3 shows that all three Gαi subunits are expressed in the chick spinal cord. Their overexpression increases cortical recruitment of LGN. Fig. S4 shows characterization of Gai1-2 and NuMA knockdown efficiency by FACS sorting and immunohistochemistry. Fig. S5 shows a summary of all constructs used in this study. Video 1: chick E3 neuroepithelial cells expressing Centrin2-GFP and H2B-GFP were imaged from the apical surface of the neuroepithelium for 5 h. Video 2: Apical view of a dividing chick E3 neuroepithelial cell expressing Centrin2-GFP. Refers to Fig. 1 a. Video 3: Z-view along the spindle axis of the same dividing cell as in Video 2. Refers to Fig. 1 b. Video 4: Chick E3 neuroepithelial cells expressing H2B-GFP were imaged from the apical surface of the neuroepithelium for 10 h. Video 5: A 3D animation depicting the biphasic spindle movements in a neuroepithelial cell during metaphase. Video 6: The same animation as in Video 5. The orange lateral belt indicates the region where the LGN complex

Table III. **Primers used for Q-RT-PCR reactions**

Amplified cDNA	Left primer	Right primer
Gαi1	5′-GAGCTGGTGAATCAGGGAAA-3′	5′-ACGTCCGCAGTCATAAATCC-3′
Gαi2	5′-ATCGTGGAGACCCACTTCAC-3′	5′-GTGCATTCGGTTCATCTCCT-3′
NuMA	5′-AGGAGCTGAGGGAGAGGAGC-3′	5′-GAGAGCTCATTCAGGGCATC-3′
GAPDH	5′-CCTCTCTGGCAAAGTCCAAG-3′	5′-CATCTGCCCATTTGATGTTG-3′

is enriched. Video 7: A 3D animation depicting the random and accelerated spindle movements during metaphase in a neuroepithelial cell with excess Gai-GDP. Compare to wild-type movements in Video 5. Video 8: A 3D animation depicting the loss of spindle movements during metaphase in a neuroepithelial cell lacking LGN or NuMA. Compare to wild-type movements in Video 5. Online supplemental material is available at http://www.jcb.org/cgi/content/full/jcb.201101039/DC1.

We thank the imaging facility of the IBDML (PICsL) and Pascal Weber for excellent technical assistance with the spinning disk microscope. We thank Marc Barad (CIML, Marseille) for assistance with FACS. We thank Drs. Quansheng Du (Medical College of Georgia) and Christian Gespach (Hopital St. Antoine, Paris) for the generous gift of plasmids.

Work performed in P. Durbec's laboratory was supported by the CNRS and a grant from the French Cancer Research Association (ARC subvention fixe) to X. Morin. Work in X. Morin's laboratory is supported by an INSERM Avenir grant and by the French Medical Research Association (FRM installation grant 2010). F. Jaouen was the recipient of pre-doctoral grants from the French Ministry for Research (MRT) and from the French Muscular Dystrophy Association (AFM). E. Peyre is the recipient of a pre-doctoral grant from the French Ministry for Research (MRT) and of the French Cancer Research Association (ARC).

The authors declare no conflicts of interest.

Submitted: 10 January 2011
Accepted: 8 March 2011

References

Aaku-Saraste, E., B. Oback, A. Hellwig, and W.B. Huttner. 1997. Neuroepithelial cells downregulate their plasma membrane polarity prior to neural tube closure and neurogenesis. *Mech. Dev.* 69:71–81. doi:10.1016/S0925-4773(97)00156-1

Adams, R.J. 1996. Metaphase spindles rotate in the neuroepithelium of rat cerebral cortex. *J. Neurosci.* 16:7610–7618.

Baena-López, L.A., A. Baonza, and A. García-Bellido. 2005. The orientation of cell divisions determines the shape of *Drosophila* organs. *Curr. Biol.* 15:1640–1644. doi:10.1016/j.cub.2005.07.062

Barnes, A.P., B.N. Lilley, Y.A. Pan, L.J. Plummer, A.W. Powell, A.N. Raines, J.R. Sanes, and F. Polleux. 2007. LKB1 and SAD kinases define a pathway required for the polarization of cortical neurons. *Cell*. 129:549–563. doi:10.1016/j.cell.2007.03.025

Bellaiche, Y., and M. Gotta. 2005. Heterotrimeric G proteins and regulation of size asymmetry during cell division. *Curr. Opin. Cell Biol.* 17:658–663. doi:10.1016/j.ceb.2005.10.002

Blumer, J.B., M.L. Bernard, Y.K. Peterson, J. Nezu, P. Chung, D.J. Dunican, J.A. Knoblich, and S.M. Lanier. 2003. Interaction of activator of G-protein signaling 3 (AGS3) with LKB1, a serine/threonine kinase involved in cell polarity and cell cycle progression: phosphorylation of the G-protein regulatory (GPR) motif as a regulatory mechanism for the interaction of GPR motifs with Gi alpha. *J. Biol. Chem.* 278:23217–23220. doi:10.1074/jbc.C200686200

Boehlke, C., F. Kotsis, V. Patel, S. Braeg, H. Voelker, S. Bredt, T. Beyer, H. Janusch, C. Hamann, M. Gödel, et al. 2010. Primary cilia regulate mTORC1 activity and cell size through Lkb1. *Nat. Cell Biol.* 12:1115–1122. doi:10.1038/ncb2117

Busson, S., D. Dujardin, A. Moreau, J. Dompierre, and J.R. De Mey. 1998. Dynein and dynactin are localized to astral microtubules and at cortical sites in mitotic epithelial cells. *Curr. Biol.* 8:541–544. doi:10.1016/S0960-9822(98)70208-8

Cabernard, C., and C.Q. Doe. 2009. Apical/basal spindle orientation is required for neuroblast homeostasis and neuronal differentiation in *Drosophila*. *Dev. Cell*. 17:134–141. doi:10.1016/j.devcel.2009.06.009

Costa, M.R., G. Wen, A. Lepier, T. Schroeder, and M. Götz. 2008. Par-complex proteins promote proliferative progenitor divisions in the developing mouse cerebral cortex. *Development*. 135:11–22. doi:10.1242/dev.009951

Du, Q., and I.G. Macara. 2004. Mammalian Pins is a conformational switch that links NuMA to heterotrimeric G proteins. *Cell*. 119:503–516. doi:10.1016/j.cell.2004.10.028

Du, Q., P.T. Stukenberg, and I.G. Macara. 2001. A mammalian Partner of inscuteable binds NuMA and regulates mitotic spindle organization. *Nat. Cell Biol.* 3:1069–1075. doi:10.1038/ncb1201-1069

Du, Q., L. Taylor, D.A. Compton, and I.G. Macara. 2002. LGN blocks the ability of NuMA to bind and stabilize microtubules. A mechanism for mitotic spindle assembly regulation. *Curr. Biol.* 12:1928–1933. doi:10.1016/S0960-9822(02)01298-8

Fischer, E., E. Legue, A. Doyen, F. Nato, J.F. Nicolas, V. Torres, M. Yaniv, and M. Pontoglio. 2006. Defective planar cell polarity in polycystic kidney disease. *Nat. Genet.* 38:21–23. doi:10.1038/ng1701

Fleming, E.S., M. Zajac, D.M. Moschenross, D.C. Montrose, D.W. Rosenberg, A.E. Cowan, and J.S. Tirnauer. 2007. Planar spindle orientation and asymmetric cytokinesis in the mouse small intestine. *J. Histochem. Cytochem.* 55:1173–1180. doi:10.1369/jhc.7A7234.2007

Fleming, E.S., M. Temchin, Q. Wu, L. Maggio-Price, and J.S. Tirnauer. 2009. Spindle misorientation in tumors from APC(min/+) mice. *Mol. Carcinog.* 48:592–598. doi:10.1002/mc.20506

Gönczy, P. 2008. Mechanisms of asymmetric cell division: flies and worms pave the way. *Nat. Rev. Mol. Cell Biol.* 9:355–366. doi:10.1038/nrm2388

Hao, Y., Q. Du, X. Chen, Z. Zheng, J.L. Balsbaugh, S. Maitra, J. Shabanowitz, D.F. Hunt, and I.G. Macara. 2010. Par3 controls epithelial spindle orientation by aPKC-mediated phosphorylation of apical Pins. *Curr. Biol.* 20:1809–1818. doi:10.1016/j.cub.2010.09.032

Haydar, T.F., E. Ang Jr., and P. Rakic. 2003. Mitotic spindle rotation and mode of cell division in the developing telencephalon. *Proc. Natl. Acad. Sci. USA*. 100:2890–2895. doi:10.1073/pnas.0437969100

Jaffe, A.B., N. Kaji, J. Durgan, and A. Hall. 2008. Cdc42 controls spindle orientation to position the apical surface during epithelial morphogenesis. *J. Cell Biol.* 183:625–633. doi:10.1083/jcb.200807121

Konno, D., G. Shioi, A. Shitamukai, A. Mori, H. Kiyonari, T. Miyata, and F. Matsuzaki. 2008. Neuroepithelial progenitors undergo LGN-dependent planar divisions to maintain self-renewability during mammalian neurogenesis. *Nat. Cell Biol.* 10:93–101. doi:10.1038/ncb1673

Kosodo, Y., K. Röper, W. Haubensak, A.M. Marzesco, D. Corbeil, and W.B. Huttner. 2004. Asymmetric distribution of the apical plasma membrane during neurogenic divisions of mammalian neuroepithelial cells. *EMBO J.* 23:2314–2324. doi:10.1038/sj.emboj.7600223

Merdes, A., K. Ramyar, J.D. Vechio, and D.W. Cleveland. 1996. A complex of NuMA and cytoplasmic dynein is essential for mitotic spindle assembly. *Cell*. 87:447–458. doi:10.1016/S0092-8674(00)81365-3

Merdes, A., R. Heald, K. Samejima, W.C. Earnshaw, and D.W. Cleveland. 2000. Formation of spindle poles by dynein/dynactin-dependent transport of NuMA. *J. Cell Biol.* 149:851–862. doi:10.1083/jcb.149.4.851

Morin, X., F. Jaouen, and P. Durbec. 2007. Control of planar divisions by the G-protein regulator LGN maintains progenitors in the chick neuroepithelium. *Nat. Neurosci.* 10:1440–1448. doi:10.1038/nn1984

Nguyen-Ngoc, T., K. Afshar, and P. Gönczy. 2007. Coupling of cortical dynein and G alpha proteins mediates spindle positioning in Caenorhabditis elegans. *Nat. Cell Biol.* 9:1294–1302. doi:10.1038/ncb1649

Noctor, S.C., V. Martínez-Cerdeño, and A.R. Kriegstein. 2008. Distinct behaviors of neural stem and progenitor cells underlie cortical neurogenesis. *J. Comp. Neurol.* 508:28–44. doi:10.1002/cne.21669

Poulson, N.D., and T. Lechler. 2010. Robust control of mitotic spindle orientation in the developing epidermis. *J. Cell Biol.* 191:915–922. doi:10.1083/jcb.201008001

Rebollo, E., P. Sampaio, J. Januschke, S. Llamazares, H. Varmark, and C. González. 2007. Functionally unequal centrosomes drive spindle orientation in asymmetrically dividing *Drosophila* neural stem cells. *Dev. Cell*. 12:467–474. doi:10.1016/j.devcel.2007.01.021

Rebollo, E., M. Roldán, and C. Gonzalez. 2009. Spindle alignment is achieved without rotation after the first cell cycle in *Drosophila* embryonic neuroblasts. *Development*. 136:3393–3397. doi:10.1242/dev.041822

Reinsch, S., and E. Karsenti. 1994. Orientation of spindle axis and distribution of plasma membrane proteins during cell division in polarized MDCKII cells. *J. Cell Biol.* 126:1509–1526. doi:10.1083/jcb.126.6.1509

Roszko, I., C. Afonso, D. Henrique, and L. Mathis. 2006. Key role played by RhoA in the balance between planar and apico-basal cell divisions in the chick neuroepithelium. *Dev. Biol.* 298:212–224. doi:10.1016/j.ydbio.2006.06.031

Rusan, N.M., and M. Peifer. 2007. A role for a novel centrosome cycle in asymmetric cell division. *J. Cell Biol.* 177:13–20. doi:10.1083/jcb.200612140

Sanada, K., and L.H. Tsai. 2005. G protein betagamma subunits and AGS3 control spindle orientation and asymmetric cell fate of cerebral cortical progenitors. *Cell*. 122:119–131. doi:10.1016/j.cell.2005.05.009

Sans, N., P.Y. Wang, Q. Du, R.S. Petralia, Y.X. Wang, S. Nakka, J.B. Blumer, I.G. Macara, and R.J. Wenthold. 2005. mPins modulates PSD-95 and SAP102 trafficking and influences NMDA receptor surface expression. *Nat. Cell Biol.* 7:1179–1190. doi:10.1038/ncb1325

Schaefer, M., M. Petronczki, D. Dorner, M. Forte, and J.A. Knoblich. 2001. Heterotrimeric G proteins direct two modes of asymmetric cell division in the *Drosophila* nervous system. *Cell*. 107:183–194. doi:10.1016/S0092-8674(01)00521-9

Sebbagh, M., M.J. Santoni, B. Hall, J.P. Borg, and M.A. Schwartz. 2009. Regulation of LKB1/STRAD localization and function by E-cadherin. *Curr. Biol.* 19:37–42. doi:10.1016/j.cub.2008.11.033

Shioi, G., D. Konno, A. Shitamukai, and F. Matsuzaki. 2009. Structural basis for self-renewal of neural progenitors in cortical neurogenesis. *Cereb. Cortex*. 19(Suppl 1):i55–i61. doi:10.1093/cercor/bhp042

Siderovski, D.P., M. Diversé-Pierluissi, and L. De Vries. 1999. The GoLoco motif: a Galphai/o binding motif and potential guanine-nucleotide exchange factor. *Trends Biochem. Sci.* 24:340–341. doi:10.1016/S0968-0004(99)01441-3

Siller, K.H., and C.Q. Doe. 2008. Lis1/dynactin regulates metaphase spindle orientation in *Drosophila* neuroblasts. *Dev. Biol.* 319:1–9. doi:10.1016/j.ydbio.2008.03.018

Théry, M., A. Jiménez-Dalmaroni, V. Racine, M. Bornens, and F. Jülicher. 2007. Experimental and theoretical study of mitotic spindle orientation. *Nature*. 447:493–496. doi:10.1038/nature05786

Willard, F.S., R.J. Kimple, and D.P. Siderovski. 2004. Return of the GDI: the GoLoco motif in cell division. *Annu. Rev. Biochem.* 73:925–951. doi:10.1146/annurev.biochem.73.011303.073756

Woodard, G.E., N.N. Huang, H. Cho, T. Miki, G.G. Tall, and J.H. Kehrl. 2010. Ric-8A and Gi alpha recruit LGN, NuMA, and dynein to the cell cortex to help orient the mitotic spindle. *Mol. Cell. Biol.* 30:3519–3530. doi:10.1128/MCB.00394-10

Yamashita, Y.M., and M.T. Fuller. 2008. Asymmetric centrosome behavior and the mechanisms of stem cell division. *J. Cell Biol.* 180:261–266. doi:10.1083/jcb.200707083

Yingling, J., Y.H. Youn, D. Darling, K. Toyo-Oka, T. Pramparo, S. Hirotsune, and A. Wynshaw-Boris. 2008. Neuroepithelial stem cell proliferation requires LIS1 for precise spindle orientation and symmetric division. *Cell*. 132:474–486. doi:10.1016/j.cell.2008.01.026

Yu, F., X. Morin, Y. Cai, X. Yang, and W. Chia. 2000. Analysis of partner of inscuteable, a novel player of *Drosophila* asymmetric divisions, reveals two distinct steps in inscuteable apical localization. *Cell*. 100:399–409. doi:10.1016/S0092-8674(00)80676-5

Yu, F., C.T. Ong, W. Chia, and X. Yang. 2002. Membrane targeting and asymmetric localization of *Drosophila* partner of inscuteable are discrete steps controlled by distinct regions of the protein. *Mol. Cell. Biol.* 22:4230–4240. doi:10.1128/MCB.22.12.4230-4240.2002

Zheng, Z., H. Zhu, Q. Wan, J. Liu, Z. Xiao, D.P. Siderovski, and Q. Du. 2010. LGN regulates mitotic spindle orientation during epithelial morphogenesis. *J. Cell Biol.* 189:275–288. doi:10.1083/jcb.200910021